Blockade of class IB phosphoinositide-3 kinase ameliorates obesity-induced inflammation and insulin resistance

Naoki Kobayashi[a], Kohjiro Ueki[a,b,1], Yukiko Okazaki[a], Aya Iwane[a], Naoto Kubota[a,b,c], Mitsuru Ohsugi[a], Motoharu Awazawa[a,c], Masatoshi Kobayashi[a], Takayoshi Sasako[a], Kazuma Kaneko[a], Miho Suzuki[a], Yoshitaka Nishikawa[a], Kazuo Hara[a], Kotaro Yoshimura[d], Isao Koshima[d], Susumu Goyama[e], Koji Murakami[f], Junko Sasaki[g], Ryozo Nagai[h], Mineo Kurokawa[e], Takehiko Sasaki[g], and Takashi Kadowaki[a,b,c,1]

[a]Department of Metabolic Diseases, [d]Department of Plastic Surgery, [e]Department of Hematology and Oncology, and [h]Department of Cardiovascular Medicine, Graduate School of Medicine, and [b]Translational Systems Biology and Medicine Initiative (TSBMI), University of Tokyo, Tokyo 113-0033, Japan; [c]Division of Applied Nutrition, National Institute of Health and Nutrition, Tokyo 162-8636, Japan; [f]Discovery Research Laboratories, Kyorin Pharmaceutical Co., Ltd., Tochigi 329-0114, Japan; and [g]Division of Microbiology, Department of Pathology and Immunology, Akita University School of Medicine, Akita 010-8543, Japan

Edited* by Lewis Clayton Cantley, Beth Israel Deaconess Medical Center, Boston, MA, and approved February 23, 2011 (received for review November 2, 2010)

Obesity and insulin resistance, the key features of metabolic syndrome, are closely associated with a state of chronic, low-grade inflammation characterized by abnormal macrophage infiltration into adipose tissues. Although it has been reported that chemokines promote leukocyte migration by activating class IB phosphoinositide-3 kinase (PI3Kγ) in inflammatory states, little is known about the role of PI3Kγ in obesity-induced macrophage infiltration into tissues, systemic inflammation, and the development of insulin resistance. In the present study, we used murine models of both diet-induced and genetically induced obesity to examine the role of PI3Kγ in the accumulation of tissue macrophages and the development of obesity-induced insulin resistance. Mice lacking p110γ (*Pik3cg*$^{-/-}$), the catalytic subunit of PI3Kγ, exhibited improved systemic insulin sensitivity with enhanced insulin signaling in the tissues of obese animals. In adipose tissues and livers of obese *Pik3cg*$^{-/-}$ mice, the numbers of infiltrated proinflammatory macrophages were markedly reduced, leading to suppression of inflammatory reactions in these tissues. Furthermore, bone marrow-specific deletion and pharmacological blockade of PI3Kγ also ameliorated obesity-induced macrophage infiltration and insulin resistance. These data suggest that PI3Kγ plays a crucial role in the development of both obesity-induced inflammation and systemic insulin resistance and that PI3Kγ can be a therapeutic target for type 2 diabetes.

Type 2 diabetes and metabolic syndrome, the major risk factors of cardiovascular disease and related death, are explosively increasing worldwide due to a pandemic of obesity that induces a variety of disorders, such as insulin resistance and hepatic steatosis (1, 2). Recent studies have revealed that obesity induces hematopoietic cell infiltration into adipose tissue, which in turn enhances adipose tissue inflammation and the secretion of proinflammatory adipokines, leading to systemic insulin resistance (3–8). Inhibition of macrophage infiltration into adipose tissue could be considered a therapeutic strategy on the basis of the accumulated evidence of obesity-related metabolic disorders.

It has been known that chemokines initiate chemotaxis by binding the corresponding G protein-coupled receptors (GPCRs), leading to activation of class IB phosphoinositide-3 kinase (PI3Kγ) (9). Upon chemokine stimulation, the unidirectional cytoskeletal rearrangement caused by PI3Kγ promotes cell movement toward the higher concentration of the chemokine. Furthermore, previous studies using mice lacking p110γ (*Pik3cg*$^{-/-}$ mice), the catalytic subunit of the PI3Kγ complex, demonstrated that PI3Kγ is essential for chemotaxis in leukocytes, including macrophages (10, 11). However, the role of PI3Kγ in obesity-induced macrophage infiltration into tissues, systemic inflammation, and the development of insulin resistance is still unknown.

To investigate the role of PI3Kγ in obesity-induced insulin resistance, we analyzed *Pik3cg*$^{-/-}$ mice fed a high-fat diet (HFD) and those with a genetically obese diabetic background and found that these mice exhibit improved insulin sensitivity along with decreased macrophage infiltration and inflammatory changes. Moreover, we have also demonstrated that a pharmacological inhibitor of PI3Kγ ameliorates obesity-induced diabetes.

Results

Mice Lacking PI3Kγ Were Protected from HFD-Induced Insulin Resistance. We fed *Pik3cg*$^{-/-}$ and wild-type control (*Pik3cg*$^{+/+}$) mice a normal diet (ND) or a HFD. While receiving ND, *Pik3cg*$^{-/-}$ mice grew normally and showed no significant differences in glucose metabolism, insulin sensitivity, and glucose tolerance compared with *Pik3cg*$^{+/+}$ mice (Fig. S1). These data suggest that PI3Kγ is not required for normal growth nor for maintenance of glucose homeostasis during ND conditions. In contrast, HFD-fed *Pik3cg*$^{-/-}$ mice maintained significantly lower blood glucose and insulin levels under random-fed conditions and also showed better response to insulin as estimated by an insulin tolerance test (ITT) (Fig. 1 *A–C*), indicating that lack of PI3Kγ led to protection from HFD-induced insulin resistance. Reflecting the improved systemic insulin sensitivity, insulin concentrations of *Pik3cg*$^{-/-}$ mice were significantly lower than those of *Pik3cg*$^{+/+}$ mice during the glucose tolerance test (GTT) whereas both groups of mice showed similar blood glucose levels (Fig. 1*D*). Furthermore, we observed significantly enhanced insulin signaling in liver and muscle of HFD-fed *Pik3cg*$^{-/-}$ mice (Fig. 1 *E* and *F* and Fig. S2). To investigate the impact of the lower weight gain of *Pik3cg*$^{-/-}$ mice compared with *Pik3cg*$^{+/+}$ mice under HFD-fed conditions without any differences in food intake and energy expenditure (Table S1), we fed *Pik3cg*$^{+/+}$ mice a limited HFD to match the weight gain of *Pik3cg*$^{-/-}$ mice. *Pik3cg*$^{-/-}$ mice still displayed better insulin sensitivity even compared with the weight-matched *Pik3cg*$^{+/+}$ mice (Fig. S3). These results suggest that PI3Kγ is required for HFD-induced systemic insulin resistance and that the body weight change does not seem to be a major cause of improved insulin sensitivity observed in HFD-fed *Pik3cg*$^{-/-}$ mice.

Author contributions: N. Kobayashi, K.U., and T.K. designed research; N. Kobayashi, K.U., Y.O., A.I., N. Kubota, M.O., M.A., M. Kobayashi, T. Sasako, K.K., M.S., Y.N., and S.G. performed research; K.Y., I.K., K.M., J.S., and T. Sasaki contributed new reagents/analytic tools; N. Kobayashi, K.U., K.H., R.N., and M. Kurokawa analyzed data; and N. Kobayashi, K.U., and T.K. wrote the paper.

The authors declare no conflict of interest.

*This Direct Submission article had a prearranged editor.

[1]To whom correspondence may be addressed. E-mail: ueki-tky@umin.ac.jp or kadowaki-3im@h.u-tokyo.ac.jp.

This article contains supporting information online at www.pnas.org/lookup/suppl/doi:10.1073/pnas.1016430108/-/DCSupplemental.

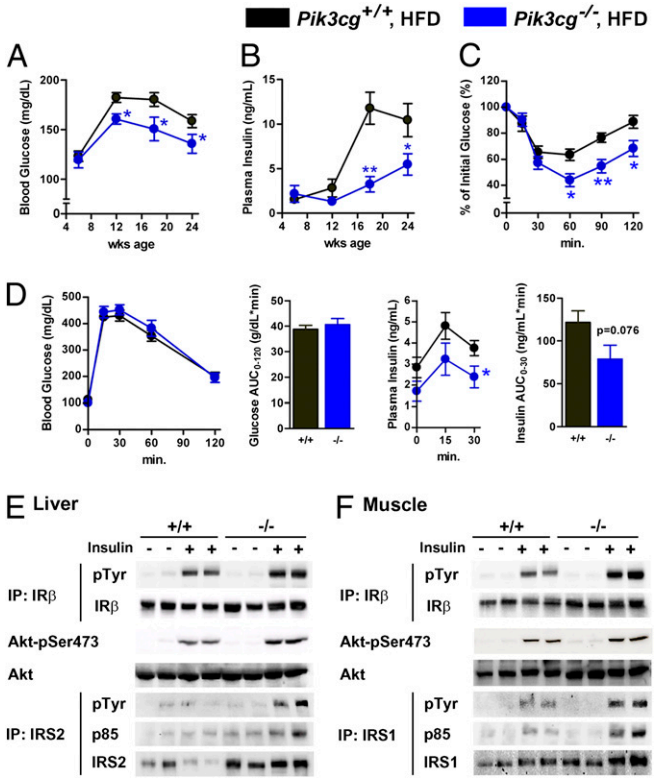

Fig. 1. Mice lacking PI3Kγ were protected from HFD-induced insulin resistance. (*A* and *B*) Blood glucose (*A*) and plasma insulin levels (*B*) in *Pik3cg*$^{+/+}$ and *Pik3cg*$^{-/-}$ mice fed on a HFD from 6 to 24 wk of age (n = 15–20). (*C*) Glucose levels during ITT (23 wk of age) were determined at the indicated time points after i.p. injection with a bolus of insulin [1.0 U·kg^{-1} body weight (BW)] (n = 7–8). (*D*) Glucose and insulin levels during GTT (24 wk of age) were determined at the indicated time points after i.p. injection with a bolus of glucose (1.5 g·kg^{-1} BW) (n = 7–8). (*E* and *F*) Phosphorylation of insulin receptor β-subunit (IRβ), insulin receptor substrate (IRS-1, IRS-2), and Akt induced by a bolus injection of insulin was assessed in livers (*E*) and skeletal muscles (*F*) of *Pik3cg*$^{+/+}$ ($^{+/+}$) and *Pik3cg*$^{-/-}$ ($^{-/-}$) mice fed a HFD (n = 3–4). IP, immunoprecipitated; pTyr, phosphorylated tyrosine; pSer, phosphorylated serine. *P < 0.05, **P < 0.01.

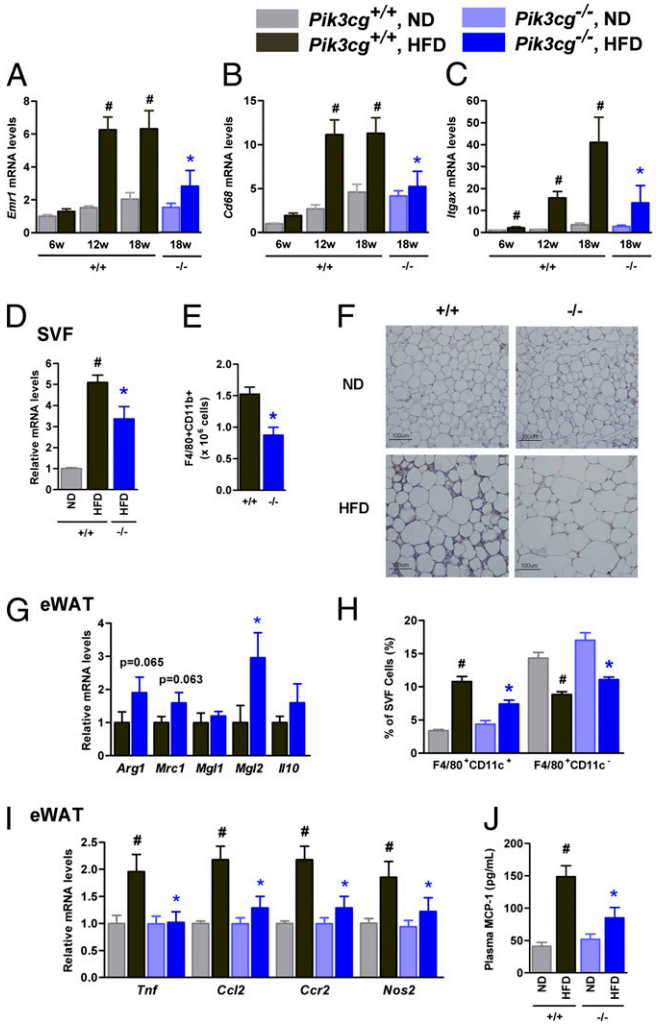

Fig. 2. Loss of PI3Kγ decreased macrophage infiltration into adipose tissue and markedly suppressed proinflammatory changes induced by a HFD. (*A*–*C*) Expression levels of *Emr1* (F4/80, *A*), *Cd68* (*B*), and *Itgax* (CD11c, *C*) in eWAT of *Pik3cg*$^{+/+}$ ($^{+/+}$) and *Pik3cg*$^{-/-}$ ($^{-/-}$) mice fed a ND or a HFD for the indicated periods (n = 6–8). (*D* and *E*) Expression levels of *Cd68* (*D*) and the population of macrophages (F4/80^{+}CD11b^{+}) measured by FACS analysis (*E*) in SVF from the eWAT (n = 4–5). (*F*) Immunohistochemical analysis of adipose tissue macrophages. eWAT of mice fed ND or HFD were stained with antibody against F4/80. (Scale bar, 100 μm.) (*G*) Expression levels of M2 macrophage-specific genes in eWAT of *Pik3cg*$^{+/+}$ and *Pik3cg*$^{-/-}$ mice fed on a HFD (normalized to *Cd68*) (n = 6–8). (*H*) Quantification of M1 macrophage (F4/80^{+}CD11c^{+}) and M2 macrophage (F4/80^{+}CD11c^{-}) in SVF from eWAT of mice fed on a ND or a HFD (n = 5). (*I*) Expression levels of proinflammatory genes in eWAT (n = 6–8). (*J*) Serum levels of MCP-1 in *Pik3cg*$^{+/+}$ and *Pik3cg*$^{-/-}$ mice fed on a ND or a HFD (n = 6–8). #P < 0.05 for HFD compared with ND. *P < 0.05 for *Pik3cg*$^{-/-}$ mice compared with *Pik3cg*$^{+/+}$ controls.

Loss of PI3Kγ Markedly Decreased the Number of Infiltrated Macrophages and the Amount of Inflammation in Adipose Tissue Induced by HFD. To clarify the mechanisms leading to the improvement of HFD-induced insulin resistance, we investigated the infiltrated macrophage contents in the epididymal adipose tissue (eWAT) of *Pik3cg*$^{-/-}$ and *Pik3cg*$^{+/+}$ mice. HFD feeding progressively increased the expression of macrophage-specific markers in the eWAT of *Pik3cg*$^{+/+}$ mice (Fig. 2 *A* and *B*). By contrast, the levels of macrophage-specific markers were markedly decreased in the eWAT, particularly in the stromal vascular fraction of *Pik3cg*$^{-/-}$ mice under HFD-fed conditions (Fig. 2 *A*, *B*, and *D*), although no significant differences in adiposity, adipocyte size, and the expression levels of genes involved in adipocyte function were observed between *Pik3cg*$^{+/+}$ and *Pik3cg*$^{-/-}$mice (Fig. S4*A* and Table S1). Fluorescence-activated cell sorting (FACS) and histological analyses also showed significant reductions of adipose tissue macrophages (ATMs) in HFD-fed *Pik3cg*$^{-/-}$ mice (Fig. 2 *E* and *F*). Expression of *Itgax* (coding CD11c), which has been reported to increase in the eWAT of mice fed a HFD (12, 13), was markedly suppressed in *Pik3cg*$^{-/-}$ mice (Fig. 2*C*). By contrast, the relative levels of genes preferentially expressed in M2 macrophages (14) were increased in the eWAT of *Pik3cg*$^{-/-}$ mice (Fig. 2*G*). FACS analysis also revealed that HFD feeding in *Pik3cg*$^{+/+}$ mice decreased the F4/80^{+}CD11c^{-} population in the stromal vascular cells of eWAT accompanied by a 3.2-fold increase in the F4/80^{+}CD11c^{+} population (Fig. 2*H*). Conversely, *Pik3cg* deletion significantly decreased the HFD-induced F4/80^{+}CD11c^{+} double-positive cells enrichment but not that of F4/80^{+}CD11c^{-} in the eWAT of HFD-fed mice (Fig. 2*H*). These changes resulted in a shift-up in the ratio of M2 to M1 macrophages in *Pik3cg*$^{-/-}$ HFD-fed mice. Because CD8^{+} T cells have recently been reported to contribute to obesity-induced inflammation in adipose tissue and systemic insulin resistance (15), we assessed the *Cd8* expression level in the eWAT of HFD-fed mice and found a small and nonsignificant reduction in the eWAT of *Pik3cg*$^{-/-}$ mice (Fig. S4*C*), suggesting that deletion of PI3Kγ more prominently affected the infiltration of M1 macrophages. To gain additional insight into the clinical importance of PI3Kγ in the fat of obese subjects, we analyzed the expression of *PIK3CG* in s.c. adipose

tissue samples of humans with a wide range of values for body mass index (BMI) (16.4–32.0). Levels of *PIK3CG* expression showed a strong correlation with BMI ($P = 0.0009$) and also correlated with *ITGAX* expression levels ($P = 0.0087$) (Fig. S5).

ATMs have been identified as the major source of inflammatory cytokine/adipokine production in the adipose tissues of obese subjects, and these chemokines are thought to be a cause of chronic inflammation and systemic insulin resistance in obesity (3). Consistent with this idea, expression levels of *Tnf*, *Ccl2*, *Ccr2*, and *Nos2* in the eWAT of HFD-fed mice were increased, whereas these increases were significantly attenuated by PI3Kγ deletion (Fig. 2*I*). Furthermore, circulating monocyte chemotactic protein-1 (MCP-1) levels also decreased with a trend toward reductions in c-jun N-terminal kinase, and IκB kinase phosphorylation in the eWAT of *Pik3cg*$^{-/-}$ mice (Fig. 2*J* and Fig. S4 *E* and *F*). Taken together, these data suggest that the loss of PI3Kγ specifically suppresses M1 macrophage infiltration, leading to suppression of HFD-induced inflammation in adipose tissue, and finally leading to improved insulin sensitivity.

However, it remained possible that deficiency of PI3Kγ would modulate insulin sensitivity through other mechanisms. Indeed, we found that elevated leptin levels observed during HFD feeding were significantly decreased with a trend to decrease *Socs3* expression by deletion of PI3Kγ (Fig. S4 *G* and *H*), suggesting improved leptin sensitivity. This could be caused by reductions of proinflammatory adipokines and also through reduced macrophage infiltration in the hypothalamus by deletion of PI3Kγ, as evidenced by deceased expression of *Emr1* (Fig. S4*H*). However, the effect appeared very limited because food intake, energy expenditure, and genes regulated by leptin were not altered by deletion of PI3Kγ.

Loss of PI3Kγ Ameliorated Diet-Induced Hepatic Steatosis. Next, we assessed the impact of PI3Kγ deficiency on HFD-induced hepatic steatosis, which is known to be tightly associated with hepatic and systemic insulin resistance (16, 17). Interestingly, hepatic triglyceride content was significantly suppressed in the livers of *Pik3cg*$^{-/-}$ mice compared with that seen in *Pik3cg*$^{+/+}$ mice, which is consistent with the histological findings by hematoxylin and eosin (H&E) staining (Fig. 3 *A* and *B*). Hepatic steatosis can be caused by overproduction of fatty acid, reduced fatty acid oxidation, increased lipid transport, and their combinations. Expression levels of genes involved in fatty acid synthesis tested here were not affected by PI3Kγ deletion (Fig. 3*C*, *Upper*), whereas *Cpt1a*, which involves fatty acid oxidation, was significantly increased in HFD-fed *Pik3cg*$^{-/-}$ mice compared with *Pik3cg*$^{+/+}$ mice (Fig. 3*C*, *Upper*). Intriguingly, expression of *Cidec* (encoding Fsp27) and *Cd36* in HFD-fed conditions was markedly suppressed in the livers of *Pik3cg*$^{-/-}$ mice (Fig. 3*C*, *Lower*). Expression of peroxisome proliferator-activated receptors (PPARγ), which is known to directly regulate *Cidec*, *Cd36*, *Scd1*, and *Pparg* itself (18–22), was also significantly decreased by deletion of PI3Kγ (Fig. 3*C*, *Lower*). Moreover, similar to findings seen with eWAT, expression of *Cd68*, *Tnf*, *Ccl2*, and its receptor *Ccr2* was significantly decreased in the livers of *Pik3cg*$^{-/-}$ mice compared with that seen in *Pik3cg*$^{+/+}$ mice (Fig. 3 *D* and *E*), and M2 macrophage markers (*Arg1*, *Mrc1*, *Mgl1*, and *Mgl2*) were up-regulated (Fig. 3*F*). The MCP-1/chemokine (C-C motif) receptor 2 (CCR2) pathway, which lies upstream of PI3Kγ, has been reported to contribute to the development of hepatic steatosis (6, 23, 24), and our findings may provide a missing link between hepatic steatosis and inflammation.

Loss of PI3Kγ in *ob/ob* Mice Reduced Inflammatory Changes in Adipose Tissue, Leading to Improvement of Insulin Sensitivity. To further assess the role of PI3Kγ in obesity-induced inflammation and insulin resistance, we generated *Pik3cg*$^{-/-}$ mice with a leptin-deficient background (*Pik3cg*$^{-/-}$*:ob/ob*). Although *Pik3cg*$^{-/-}$*:ob/ob* mice gained body weight in a similar manner compared with *Pik3cg*$^{+/+}$*:ob/ob* mice, they displayed lower blood glucose levels up to 20 wk of age (Fig.4 *A* and *B*). Similarly, *Pik3cg*$^{-/-}$*:ob/ob* mice also displayed significantly decreased glucose levels in a fasted state as well as during ITT and GTT (Fig. 4 *C* and *D*) along with enhanced insulin-stimulated Akt (also known as protein kinase B or PKB) phosphorylation in both liver and muscle

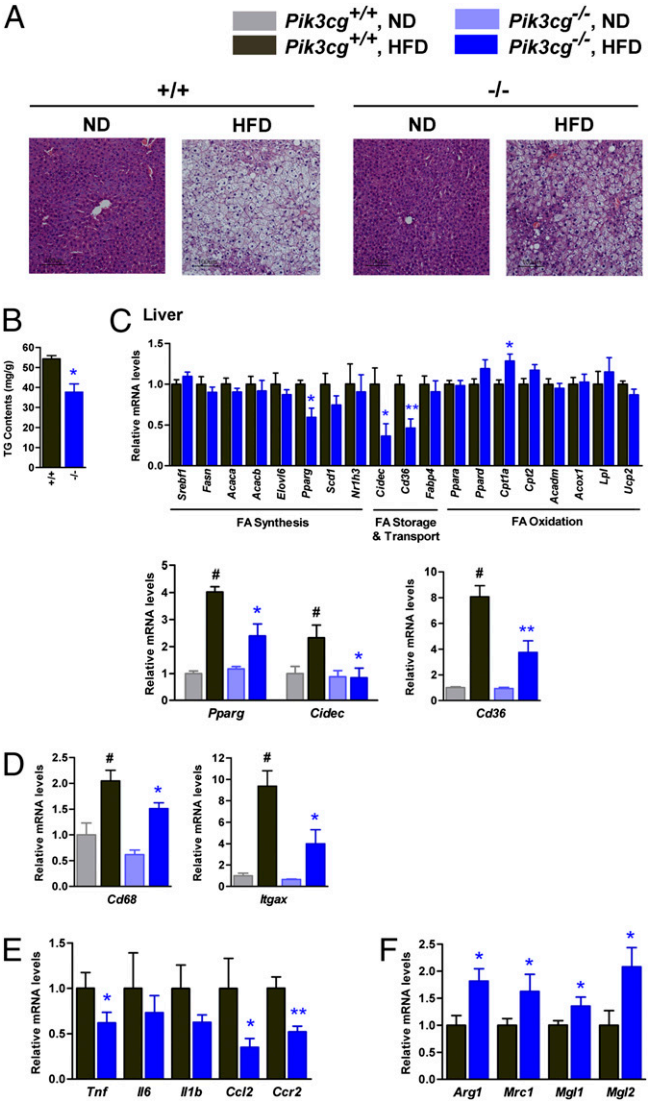

Fig. 3. PI3Kγ knockout mice showed amelioration of HFD-induced hepatic steatosis. (*A*) Hematoxylin and eosin-stained sections of liver from *Pik3cg*$^{+/+}$ ($^{+/+}$) and *Pik3cg*$^{-/-}$ ($^{-/-}$) mice on a ND or a HFD. (Scale bar, 100 μm.) (*B*) Triglyceride (TG) content in liver of mice on a HFD ($n = 7$–8). (*C*) Expression levels of mRNA related to fatty acid metabolism in liver of fasted mice ($n = 7$–8). (*D*–*F*) Expression levels of genes encoded macrophage-related protein (*D*), proinflammatory genes (*E*), and M2 macrophage-specific genes (normalized to *Cd68*, *F*) in liver ($n = 7$–8). #$P < 0.05$ for a HFD compared with ND. *$P < 0.05$ and **$P < 0.01$ for *Pik3cg*$^{-/-}$ mice compared with *Pik3cg*$^{+/+}$ controls.

of *Pik3cg*$^{-/-}$*:ob/ob* mice (Fig. 4*E*). In addition, the expression of *Emr1*, *Cd68*, and *Tnf* in the eWAT of *Pik3cg*$^{-/-}$*:ob/ob* mice was also significantly decreased (Fig. 4 *F* and *G*), whereas M2 macrophage markers were up-regulated (Fig. 4*H*). These data suggest that loss of PI3Kγ ameliorated obesity-induced insulin resistance through the reduction of macrophage infiltration and inflammation even in a genetically obese model and that a large part of these beneficial effects of PI3Kγ deficiency on glucose metabolism appears to be independent of leptin signaling and body weight change.

Bone Marrow-Specific Deletion of PI3Kγ Ameliorates Obesity-Induced Diabetes. Although PI3Kγ is almost exclusively expressed in hematopoietic cells, to rule out the possibility that PI3Kγ in extrahematopoietic parenchymal tissues might play some role in glucose metabolism, we generated a bone marrow (BM)-specific PI3Kγ deletion in *ob/ob* [*Pik3cg*$^{-/-}$ bone marrow transplant

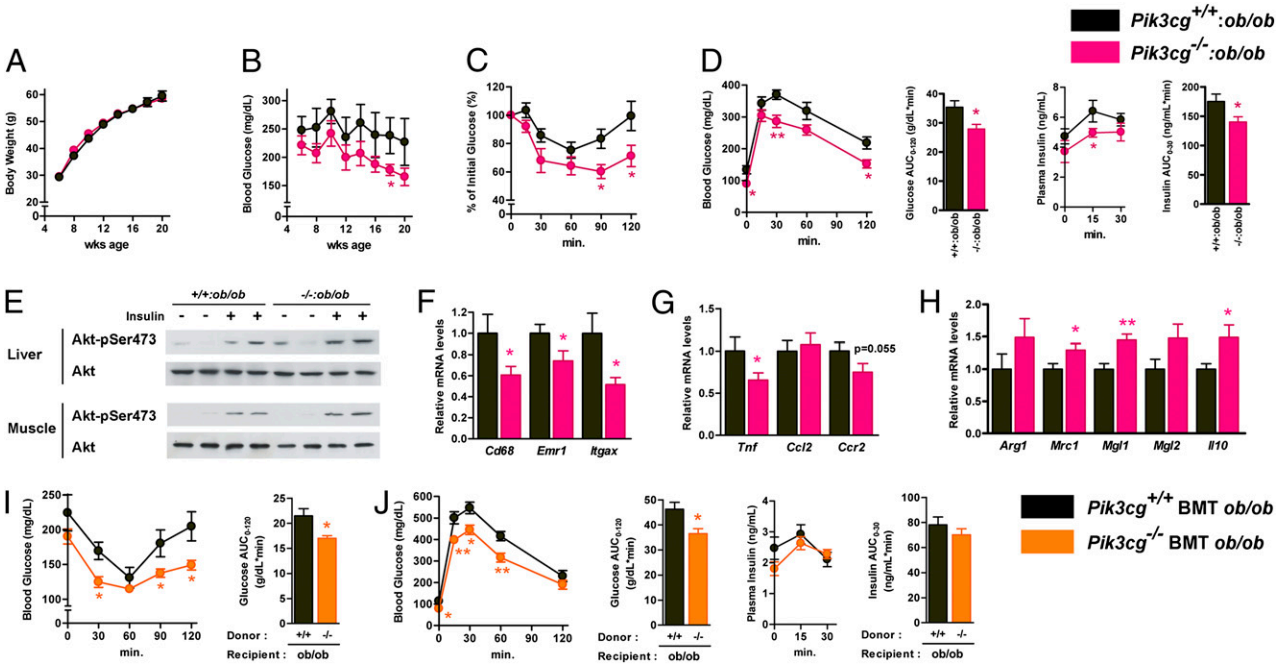

Fig. 4. Loss of PI3Kγ in the *ob/ob* background improved insulin sensitivity. (*A* and *B*) Time course of body weight (*A*) and blood glucose (*B*) in *Pik3cg*$^{+/+}$*:ob/ob* and double-mutant *Pik3cg*$^{-/-}$*:ob/ob* mice (n = 12–18). (*C*) Glucose levels during ITT (8 wk of age) were determined at the indicated time points after i.p. injection with a bolus of insulin (2.0 U·kg^{-1} BW) (n = 7–8). (*D*) Glucose and insulin levels during GTT (9 wk of age) were determined at the indicated time points after i.p. injection with a bolus of glucose (1.0 g·kg^{-1} BW) (n = 7–8). (*E*) Phosphorylation of Akt in livers and skeletal muscles induced by a bolus injection of insulin was assessed. (*F–H*) Expression levels of genes encoded macrophage-related protein (*F*), proinflammatory genes (*G*), and M2 macrophage-specific genes (normalized to *Cd68*, *H*) in eWAT (n = 7–8). (*I* and *J*) Bone marrow-specific PI3Kγ knockout *ob/ob* mice were generated by bone marrow transplantation. (*I*) Glucose levels during ITT were determined at the indicated time points after i.p. injection with a bolus of insulin (2.0 U·kg^{-1} BW). (*J*) Glucose and insulin levels during GTT were determined at the indicated time points after i.p. injection with a bolus of glucose (1.0 g·kg^{-1} BW) (n = 6). $^{*}P < 0.05$, $^{**}P < 0.01$.

(BMT) *ob/ob*] mice by BM transplantation. Compared with the control mice that received the *Pik3cg*$^{+/+}$ BM cells, *Pik3cg*$^{-/-}$ BMT *ob/ob* mice displayed improved glucose levels, systemic insulin sensitivity, and glucose intolerance (Fig. 4 *I* and *J*), as observed in *ob/ob* mice systemically lacking *Pik3cg*$^{-/-}$. These data strongly suggest that the metabolic phenotypes of *Pik3cg*$^{-/-}$*:ob/ob* mice are mainly owing to the lack of PI3Kγ in BM-derived cells. Moreover, we also confirmed that BM-specific *Pik3cg*$^{-/-}$ (*Pik3cg*$^{-/-}$ BMT) mice fed a HFD exhibited the phenotypes similar to those of mice systemically lacking *Pik3cg*$^{-/-}$ (Fig. S6). Furthermore, the in vitro studies revealed that lack of PI3Kγ did not significantly alter expression of *Itgax* in BM-derived macrophages (BMDM), induction of *Mgl2* in IL-4–stimulated alternative activation in BMDM, or LPS-stimulated proinflammatory cytokine expression in peritoneal macrophages (Fig. S7 *A–C*).

Blockade of PI3Kγ by a Pharmacological Inhibitor Ameliorated Obesity-Induced Diabetes. Finally, we addressed whether pharmacological inhibition of PI3Kγ could ameliorate insulin resistance in obese diabetic animal models using AS-605240, a small-molecule inhibitor for PI3Kγ (25). We confirmed that AS-605240 selectively blocked class IB PI3K signaling in cultured macrophages (Fig. S7*D*), as shown in the previous reports (26, 27). Treatment with 10 mg/kg/d of AS-605240 lowered blood glucose levels, with an associated significant improvement of both insulin sensitivity and glucose tolerance (Fig. 5 *A–C*) without affecting body weight (54.2 ± 0.8 g for vehicle, 54.0 ± 0.5 g for 10 mg/kg/d of AS-605240). A total of 30 mg/kg/d of AS-605240 displayed more profound effects (Fig. 5 *A–C*) with slightly less weight gain (49.5 ± 0.8 g). Moreover, AS-605240 dose-dependently reduced the abundance of ATMs as estimated by F4/80 staining and the expression levels of macrophage markers in eWAT (Fig. 5 *D* and *E*). As a consequence, the circulating levels of MCP-1 were also reduced in *ob/ob* mice treated with AS-605240 (Fig. 5*F*). We also confirmed that *Pik3cg*$^{+/+}$ mice fed a HFD treated with AS-605240 exhibited metabolic phenotypes very similar to those of *Pik3cg*$^{-/-}$ mice (Fig. S8). These findings strongly suggest that pharmacological intervention by inhibiting PI3Kγ is effective even after establishment of a morbidly obese condition.

Discussion

Obesity causes a variety of metabolic disorders, including diabetes and fatty liver disease, initiated by macrophage infiltration into adipose tissue and presumably also into liver. Previous studies have shown that MCP-1 triggers this macrophage infiltration and that modulation of the MCP-1/CCR2 signaling by genetic disruption or treatment with an inhibitory molecule can ameliorate obesity-induced insulin resistance (5, 6, 23, 24, 28). Other chemokines have recently been suggested to also promote macrophage infiltration in obesity (8, 29, 30). Receptors for these chemokines, including CCR2, are GPCRs, of which PI3Kγ lies downstream and mediates the signal to promote cell movement in response to chemokine stimulation (10, 11, 31, 32). Here, we show that suppression of PI3Kγ activity attenuates obesity-induced proinflammatory macrophage infiltration into adipose tissue and liver, leading to improvement of insulin resistance.

HFD feeding markedly increases CD11c-positive macrophages in eWAT as well as in the liver of *Pik3cg*$^{+/+}$ mice, whereas the increase is significantly suppressed by disruption of PI3Kγ. By contrast, the expression of the M2 macrophage marker is not decreased in these tissues of *Pik3cg*$^{-/-}$ mice fed a HFD, leading to an increase in the ratio of M2 to M1. This is because M1 macrophages, but not M2 macrophages, abundantly express CCR2 that promotes cell migration into both adipose tissue and liver via PI3Kγ activation. Furthermore, the results of BMT experiments using *ob/ob* or HFD-fed mice clearly demonstrate that the improved glucose metabolism caused by a lack of PI3Kγ is largely attributed to BM cells. Together with the results of in vitro experiments, the improved insulin sensitivity and glucose homeostasis associated with decreased inflammatory changes in the adipose tissue and liver of obese *Pik3cg*$^{-/-}$ mice

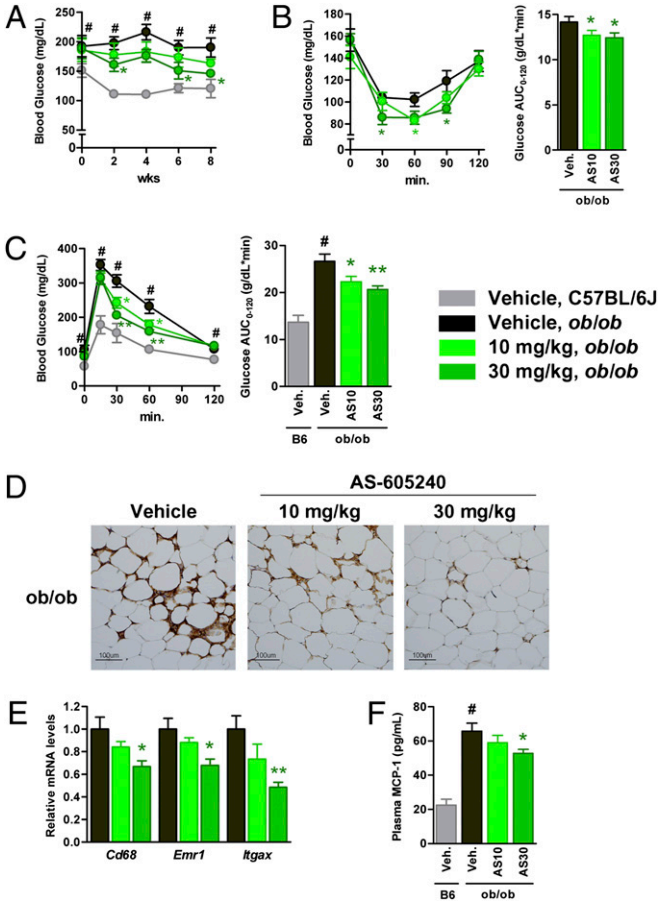

Fig. 5. Blockade of PI3Kγ by a pharmacological inhibitor ameliorated diabetes in *ob/ob* mice. *ob/ob* mice were treated with a PI3Kγ inhibitor, AS-605240, from 6 wk of age for 8 wk. Age-matched C57BL/6J mice served as lean controls. (*A*) Time course of blood glucose levels in vehicle, 10 or 30 mg/kg/d of AS-605240–treated *ob/ob* mice (designated as AS10 or AS30, respectively), and vehicle-treated C57BL/6J mice. (*B* and *C*) Glucose levels during ITT (7 wk treatment, *B*) or GTT (8 wk treatment, *C*) in vehicle (Veh.) or AS-605240–treated *ob/ob* mice were determined at the indicated time points after i.p. injection with a bolus of insulin (1.0 $U \cdot kg^{-1}$ BW) for ITT or glucose (1.5 $g \cdot kg^{-1}$ BW) for GTT. (*D*) Immunohistochemical analysis of adipose tissue macrophage. eWAT of *ob/ob* mice treated with vehicle or AS-605240 were stained with antibody against F4/80. (Scale bar, 100 μM.) (*E*) Expression levels of genes encoded macrophage-related protein in eWAT of vehicle or AS-605240–treated *ob/ob* mice. (*F*) Serum MCP-1 levels in vehicle or AS-605240–treated *ob/ob* mice and vehicle-treated C57BL/6J mice. (n = 7–8). #$P < 0.05$ for vehicle-treated *ob/ob* compared with vehicle-treated C57BL/6J mice. *$P < 0.05$ and **$P < 0.01$ for AS-605240–treated *ob/ob* compared with vehicle-treated *ob/ob* control.

are largely due to a reduction in the number of infiltrated M1 macrophages that produce proinflammatory adipokines, which thereby promotes systemic insulin resistance, but not the functional changes or differentiation defects in these cells.

Hepatic steatosis is also known to exacerbate insulin resistance in obesity and cause liver dysfunction, such as nonalcoholic steatohepatitis (33). In the liver of *Pik3cg*$^{-/-}$ mice, expression of *Pparg* and *Cidec* is significantly decreased without any alterations in genes involved in fatty acid synthesis, whereas genes regulating β-oxidation, such as *Cpt1a*, are up-regulated, consistent with the previous report that Fsp27 suppresses β-oxidation and triglyceride turnover in hepatocytes (21). Fsp27 has been reported to regulate lipid droplet formation downstream of PPARγ in adipocytes, and deletion of Fsp27 leads to protection from diet-induced obesity (22), although it is unclear whether Fsp27 also functions as a key regulator of lipid droplet formation in hepatocytes. Meanwhile, PPARγ expression levels in the eWAT of *Pik3cg*$^{-/-}$ mice are not suppressed differently from those in liver. It is proposed that, when the capacity of lipid storage in adipose tissue, presumably regulated by PPARγ, reaches a limit, accumulation of lipids in extra-adipose tissue, such as liver and muscle, takes place, leading to insulin resistance (1, 16). Moreover, it has been suggested that suppression of inflammation reduces the development of hepatic steatosis and insulin resistance. Indeed, treatment with a CCR2 inhibitor ameliorates insulin resistance and hepatic steatosis in *db/db* mice associated with significant reductions in the expression of CD36 in liver (23). Although it remains unclear how PI3Kγ deficiency causes the suppression of lipid accumulation in liver, it is possible that inhibition of macrophage infiltration into adipose tissue and liver, and the subsequent reduction of inflammatory changes, can decrease PPARγ expression in liver but not in adipocytes. This may inhibit the ectopic lipid accumulation, leading to systemic insulin sensitivity, although it should be explored how PPARγ is regulated in these tissues.

Inhibitors for PI3Kδ and PI3Kγ are expected to be therapeutic agents for chronic inflammatory diseases (34, 35). Indeed, pharmacological inhibition of PI3Kγ ameliorates rheumatoid arthritis, lupus nephritis, and atherosclerosis in mouse models (25, 27, 34, 36), and here we provide evidence that the PI3Kγ inhibition is also promising for treatment of obesity-induced diabetes. Because multiple chemokine-signaling pathways can be involved in macrophage infiltration and inflammation in an obese context, and because inhibition of PI3Kγ could suppress macrophage migration caused by all these chemokines (8, 34), blockade of PI3Kγ appears to have advantages compared with the strategies to inhibit single chemokine signaling, such as MCP-1 or CCR2, which have been shown to improve insulin sensitivity in obese mice (6, 23, 28). However, a highly selective inhibitor for PI3Kγ, which does not affect class IA PI3Ks and other kinases, should be developed and carefully evaluated for clinical use to avoid potential adverse effects, such as inhibition of insulin signaling. Nevertheless, our data suggest that PI3Kγ inhibition can be a strategy for treating obesity-induced insulin resistance.

We have clearly demonstrated that PI3Kγ plays a crucial role in obesity-induced inflammation, hepatic steatosis, and systemic insulin resistance and that inhibition of PI3Kγ activity ameliorates obesity-induced insulin resistance, at least in part, due to the reductions in macrophage infiltration and subsequent inflammatory responses in both adipose tissue and liver. These findings provide a possibility for a therapeutic approach to obesity-induced diabetes and fatty liver disease.

Materials and Methods

Mice. We generated *Pik3cg*$^{-/-}$ mice as previously described (11) and used these mice after they were backcrossed to C57BL/6J mice for more than 16 generations with C57BL/6J mice as the controls. *Pik3cg*$^{-/-}$:*ob/ob* mice were generated by intercrossing *Pik3cg*$^{+/-}$:*ob/+* mice. All mice were housed under a 12-h light/12-h dark cycle and had free access to sterile water and pellet food ad libitum except when fed a limited HFD. The animal care and experimental procedures were approved by the Animal Care Committee of the University of Tokyo.

Metabolic Studies. Male *Pik3cg*$^{-/-}$ and *Pik3cg*$^{+/+}$ mice were fed a standard chow (CE-2; CLEA Japan) or high-fat/high-caloric diet (high fat diet 32; CLEA Japan). For ITTs, mice received i.p. injections of human insulin (Humalin R; Eli Lilly) in the ad libitum feeding state. For GTTs, mice received i.p. injections of glucose after an overnight fast. Blood glucose levels were measured using a Glutest sensor (Sanwa Chemical) at the indicated time points, and the plasma insulin levels were measured using a RIA kit (Biotrek), as previously described (37).

Insulin-Signaling Analysis. Mice were anesthetized after 16 h of fasting, and human insulin was injected into the inferior vena cava. After 5 min, tissues were quickly excised and frozen in liquid nitrogen. Tissue lysates were prepared and used for immunoprecipitation and immunoblotting as previously described (38).

Gene Expression Analysis. TRIzol reagent (Invitrogen) was used to prepare total RNA from tissues. The reverse-transcription reaction was carried out with a high-capacity cDNA reverse transcription kit (Applied Biosystems). Quantitative PCR analyses using TaqMan assays were performed as previously described (37). The relative expression levels were normalized by measurement of the amount of cyclophilin in each sample.

Histological Analysis. Tissue samples for histology were fixed in 4% paraformaldehyde in PBS overnight, and paraffin-embedded sections were prepared (4-μm sections). Sections of liver were stained with H&E, and adipose tissues were stained hematoxylin and incubated with anti-F4/80 (1:20; Serotec) overnight at 4 °C, followed by incubation with the Vectastain Elite ABC Rat IgG Kit and visualization with the ImmPACT DAB Substrate Kit (Vector Laboratories), as previously described (5).

Adipose Tissue Fractionation and FACS Analysis. Adipose tissue fractionation into the stromal vascular fraction (SVF) was performed as previously described (5). Briefly, epididymal adipose tissue pads were minced into fine pieces and centrifuged at 3,000 × *g* to remove erythrocytes and free leukocytes. Tissues were incubated with 2 mg/mL of collagenase type 2 (Worthington) at 37 °C with gentle agitation for 15–20 min. Digested tissues were filtered through nylon mesh (100 μm), and the filtrate was centrifuged at 1,200 × *g*. Pelleted cells were collected as the SVF. For isolation of mRNA, the erythrocyte-depleted SVF was resuspended in TRIzol reagent (Invitrogen). For flow cytometric analysis, after removing red blood cells, the SVF was incubated with either labeled monoclonal antibody or isotype control antibody and analyzed by flow cytometry using a FACS Calibur (Becton Dickinson). Data acquisition and analysis were performed using CellQuest Pro software (Becton Dickinson). Propidium iodide was used to exclude dead cells.

Plasma MCP-1 and Hepatic Triglyceride Content. Plasma levels for MCP-1 were measured by ELISA (R&D Systems). Hepatic triglyceride was extracted from the liver homogenate with Folchsolutioin (chloroform:methanol = 2:1, vol/vol). An aliquot of the organic phase was collected and resuspended in ethanol containing 1% Triton X-100 and then measured by enzyme-based measurement kits (Roche Diagnostics).

Bone Marrow Transplantation. For BM transplant studies, bone marrow cells were prepared from the femur and tibia of *Pik3cg*$^{+/+}$ and *Pik3cg*$^{-/-}$ mice and injected i.v. (5×10^6 cells/recipient) into lethally irradiated *ob/ob* mice or C57BL/6J mice (7.0 Gy) as recipients, as described previously (39, 40).

Treatment with a PI3Kγ Inhibitor. A PI3Kγ selective inhibitor, AS-605240, which was synthesized by Discovery Research Laboratories, Kyorin Pharmaceutical, was used as described previously (25). Vehicle or AS-605240 was administered intraperitoneally to *ob/ob* mice twice a day from 6 wk of age.

Statistical Analysis. Values of the data are expressed as mean ± SEM. Differences between two groups were assessed using unpaired two-tailed *t* tests. Data involving more than two groups were assessed by analysis of variance. Statistical significance is displayed as $P < 0.05$ (one asterisk) or $P < 0.01$ (two asterisks) in figures.

ACKNOWLEDGMENTS. We thank R. Hoshino, F. Takahashi, Y. Kanto, and Y. Kishida for their excellent technical assistance. This work was supported by a grant for the Translational Systems Biology and Medicine Initiative from the Ministry of Education, Culture, Sports, Science and Technology of Japan (to T.K.), a Grant-in-Aid for Scientific Research in Priority Areas (S) from the Ministry of Education, Culture, Sports, Science and Technology of Japan (to T.K.), a Grant-in-Aid for Scientific Research in Priority Areas (B) from the Ministry of Education, Culture, Sports, Science and Technology of Japan (to K.U.), a Grant-in-Aid for Scientific Research from the Ministry of Health, Labor and Welfare (to K.U.), Health Science Research grants (Research on Human Genome and Gene Therapy) from the Ministry of Health and Welfare (to T.K.), and a grant from Takeda Science Foundation (to K.U.).

1. Kahn SE, Hull RL, Utzschneider KM (2006) Mechanisms linking obesity to insulin resistance and type 2 diabetes. *Nature* 444:840–846.
2. Yach D, Stuckler D, Brownell KD (2006) Epidemiologic and economic consequences of the global epidemics of obesity and diabetes. *Nat Med* 12:62–66.
3. Weisberg SP, et al. (2003) Obesity is associated with macrophage accumulation in adipose tissue. *J Clin Invest* 112:1796–1808.
4. Xu H, et al. (2003) Chronic inflammation in fat plays a crucial role in the development of obesity-related insulin resistance. *J Clin Invest* 112:1821–1830.
5. Kamei N, et al. (2006) Overexpression of monocyte chemoattractant protein-1 in adipose tissues causes macrophage recruitment and insulin resistance. *J Biol Chem* 281:26602–26614.
6. Kanda H, et al. (2006) MCP-1 contributes to macrophage infiltration into adipose tissue, insulin resistance, and hepatic steatosis in obesity. *J Clin Invest* 116:1494–1505.
7. Zeyda M, et al. (2007) Human adipose tissue macrophages are of an anti-inflammatory phenotype but capable of excessive pro-inflammatory mediator production. *Int J Obes (Lond)* 31:1420–1428.
8. Chavey C, et al. (2009) CXC ligand 5 is an adipose-tissue derived factor that links obesity to insulin resistance. *Cell Metab* 9:339–349.
9. Oak JS, Matheu MP, Parker I, Cahalan MD, Fruman DA (2007) Lymphocyte cell motility: The twisting, turning tale of phosphoinositide 3-kinase. *Biochem Soc Trans* 35:1109–1113.
10. Hirsch E, et al. (2000) Central role for G protein-coupled phosphoinositide 3-kinase gamma in inflammation. *Science* 287:1049–1053.
11. Sasaki T, et al. (2000) Function of PI3Kgamma in thymocyte development, T cell activation, and neutrophil migration. *Science* 287:1040–1046.
12. Lumeng CN, Bodzin JL, Saltiel AR (2007) Obesity induces a phenotypic switch in adipose tissue macrophage polarization. *J Clin Invest* 117:175–184.
13. Lumeng CN, DelProposto JB, Westcott DJ, Saltiel AR (2008) Phenotypic switching of adipose tissue macrophages with obesity is generated by spatiotemporal differences in macrophage subtypes. *Diabetes* 57:3239–3246.
14. Gordon S (2003) Alternative activation of macrophages. *Nat Rev Immunol* 3:23–35.
15. Nishimura S, et al. (2009) CD8+ effector T cells contribute to macrophage recruitment and adipose tissue inflammation in obesity. *Nat Med* 15:914–920.
16. Després JP, Lemieux I (2006) Abdominal obesity and metabolic syndrome. *Nature* 444: 881–887.
17. Perlemuter G, Bigorgne A, Cassard-Doulcier AM, Naveau S (2007) Nonalcoholic fatty liver disease: From pathogenesis to patient care. *Nat Clin Pract Endocrinol Metab* 3: 458–469.
18. Tontonoz P, Spiegelman BM (2008) Fat and beyond: The diverse biology of PPARgamma. *Annu Rev Biochem* 77:289–312.
19. Bouhlel MA, et al. (2007) PPARgamma activation primes human monocytes into alternative M2 macrophages with anti-inflammatory properties. *Cell Metab* 6: 137–143.
20. Odegaard JI, et al. (2007) Macrophage-specific PPARgamma controls alternative activation and improves insulin resistance. *Nature* 447:1116–1120.
21. Matsusue K, et al. (2008) Hepatic steatosis in leptin-deficient mice is promoted by the PPARgamma target gene Fsp27. *Cell Metab* 7:302–311.
22. Nishino N, et al. (2008) FSP27 contributes to efficient energy storage in murine white adipocytes by promoting the formation of unilocular lipid droplets. *J Clin Invest* 118: 2808–2821.
23. Tamura Y, et al. (2008) Inhibition of CCR2 ameliorates insulin resistance and hepatic steatosis in db/db mice. *Arterioscler Thromb Vasc Biol* 28:2195–2201.
24. Yang SJ, Iglayreger HB, Kadouh HC, Bodary PF (2009) Inhibition of the chemokine (C-C motif) ligand 2/chemokine (C-C motif) receptor 2 pathway attenuates hyperglycaemia and inflammation in a mouse model of hepatic steatosis and lipoatrophy. *Diabetologia* 52:972–981.
25. Barber DF, et al. (2005) PI3Kgamma inhibition blocks glomerulonephritis and extends lifespan in a mouse model of systemic lupus. *Nat Med* 11:933–935.
26. Guillermet-Guibert J, et al. (2008) The p110beta isoform of phosphoinositide 3-kinase signals downstream of G protein-coupled receptors and is functionally redundant with p110gamma. *Proc Natl Acad Sci USA* 105:8292–8297.
27. Camps M, et al. (2005) Blockade of PI3Kgamma suppresses joint inflammation and damage in mouse models of rheumatoid arthritis. *Nat Med* 11:936–943.
28. Weisberg SP, et al. (2006) CCR2 modulates inflammatory and metabolic effects of high-fat feeding. *J Clin Invest* 116:115–124.
29. Huber J, et al. (2008) CC chemokine and CC chemokine receptor profiles in visceral and subcutaneous adipose tissue are altered in human obesity. *J Clin Endocrinol Metab* 93:3215–3221.
30. Nara N, et al. (2007) Disruption of CXC motif chemokine ligand-14 in mice ameliorates obesity-induced insulin resistance. *J Biol Chem* 282:30794–30803.
31. Ferguson GJ, et al. (2007) PI(3)Kgamma has an important context-dependent role in neutrophil chemokinesis. *Nat Cell Biol* 9:86–91.
32. Nishio M, et al. (2007) Control of cell polarity and motility by the PtdIns(3,4,5)P3 phosphatase SHIP1. *Nat Cell Biol* 9:36–44.
33. Nugent C, Younossi ZM (2007) Evaluation and management of obesity-related nonalcoholic fatty liver disease. *Nat Clin Pract Gastroenterol Hepatol* 4:432–441.
34. Rückle T, Schwarz MK, Rommel C (2006) PI3Kgamma inhibition: Towards an 'aspirin of the 21st century'? *Nat Rev Drug Discov* 5:903–918.
35. Marone R, Cmiljanovic V, Giese B, Wymann MP (2008) Targeting phosphoinositide 3-kinase: Moving towards therapy. *Biochim Biophys Acta* 1784:159–185.
36. Chang JD, et al. (2007) Deletion of the phosphoinositide 3-kinase p110gamma gene attenuates murine atherosclerosis. *Proc Natl Acad Sci USA* 104:8077–8082.
37. Kubota N, et al. (2008) Dynamic functional relay between insulin receptor substrate 1 and 2 in hepatic insulin signaling during fasting and feeding. *Cell Metab* 8:49–64.
38. Ueki K, et al. (2002) Increased insulin sensitivity in mice lacking p85β subunit of phosphoinositide 3-kinase. *Proc Natl Acad Sci USA* 99:419–424.
39. Goyama S, et al. (2008) Evi-1 is a critical regulator for hematopoietic stem cells and transformed leukemic cells. *Cell Stem Cell* 3:207–220.
40. Ito A, et al. (2008) Role of CC chemokine receptor 2 in bone marrow cells in the recruitment of macrophages into obese adipose tissue. *J Biol Chem* 283: 35715–35723.